JPE 13-5-10

http://dx.doi.org/10.6113/JPE.2013.13.5.829

A Single-Input Single-Output Approach by using Minor-Loop Voltage Feedback Compensation with Modified SPWM Technique for Three-Phase AC–DC Buck Converter

Azrita Alias[†*], Nasrudin Abd. Rahim[*,**], and Mohamed Azlan Hussain[*]

[†]Faculty of Electrical Eng., Universiti Teknikal Malaysia Melaka (UTeM), Melaka, Malaysia
[*]UM Power Energy Dedicated Advanced Centre (UMPEDAC), University of Malaya, Kuala Lumpur, Malaysia
[**]King Abdulaziz University, Jeddah, Saudi Arabia

Abstract

The modified sinusoidal pulse-width modulation (SPWM) is one of the PWM techniques used in three-phase AC–DC buck converters. The modified SPWM works without the current sensor (the converter is current sensorless), improves production of sinusoidal AC current, enables obtainment of near-unity power factor, and controls output voltage through modulation gain (ranging from 0 to 1). The main problem of the modified SPWM is the huge starting current and voltage (during transient) that results from a large step change from the reference voltage. When the load changes, the output voltage significantly drops (through switching losses and non-ideal converter elements). The single-input single-output (SISO) approach with minor-loop voltage feedback controller presented here overcomes this problem. This approach is created on a theoretical linear model and verified by discrete-model simulation on MATLAB/Simulink. The capability and effectiveness of the SISO approach in compensating start-up current/voltage and in achieving zero steady-state error were tested for transient cases with step-changed load and step-changed reference voltage for linear and non-linear loads. Tests were done to analyze the transient performance against various controller gains. An experiment prototype was also developed for verification.

Key words: MATLAB-Simulink, Minor-loop feedback compensator, Modified SPWM, Three-phase AC–DC buck converter

I. INTRODUCTION

Three-phase AC–DC buck converters have obtained high interest for telecommunication equipment (front-end converters), motor drives, uninterruptible power supply systems, and power supply for process technologies. Switch-mode configurations, which replace conventional diode-rectifiers, have been extensively developed to overcome the disadvantages of conventional diode-rectifiers, including poor line power and high harmonic content on the grid. Various switching control strategies for three-phase power converters have been discussed [1]–[8]. These strategies include hysteresis current mode control, average current mode control, carrier-based pulse-width modulation (PWM), predictive current-control technique, and space vector modulation. The main objective of these studies is to improve the AC–DC input current wave-shape (into near-sinusoidal shape) while obtaining unity power factor to comply with governmental and international standards, such as IEEE 519, IEC-1000, and IEC 61000-3-2 [9], [10].

The most recognized technique is PWM, which has simple control and a wide range of application. The application of PWM has been reported in [11]. Utilizing the PWM improves the power quality of AC–DC power converters. The authors in [12] conclude that PWM regenerative rectifiers are highly developed, the technology is mature, and their industry acceptance is wide. The simplest PWM technique is

Manuscript received Mar. 25, 2013; revised Jun. 28, 2013
Recommended for publication by Associate Editor Jun-Keun Ji.
[†]Corresponding Author: azrita@utem.edu.my
Tel: +603-2246 3246, Fax: +603-2246 3257, University of Malaya
[*]UM Power Energy Dedicated Advanced Centre (UMPEDAC), University of Malaya, Malaysia

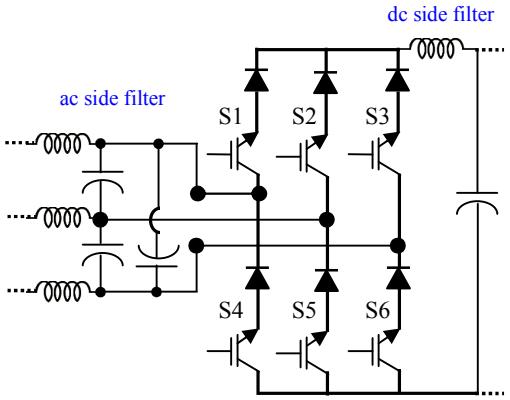

Fig. 1 Ac-dc buck converter (6-switch 6-diodes)

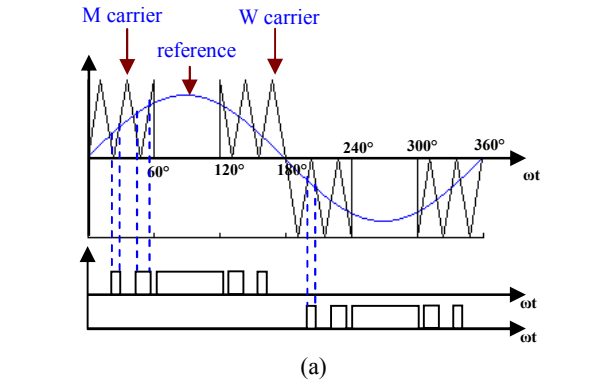

(a)

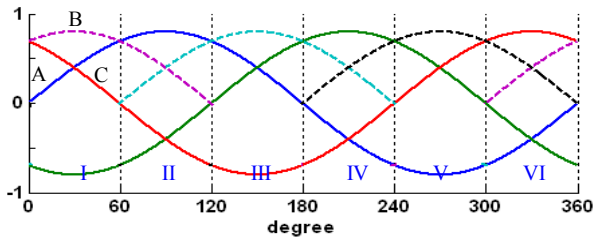

(b)

Fig. 2. (a) The illustration of generating modified SPWM. (b) Six section of three-phase supply-voltage waveforms, showing a similar pattern in each section.

carrier-based PWM, which is used at fixed frequency in which the modulating signals are controlled by varying the duty cycle. Modified sinusoidal pulse-width modulation (SPWM) is a carrier-based PWM that is suitable for three-phase AC–DC buck converter application. Theoretically, the switching technique uses two types of carrier signals ("M" and "W" shapes) and 1/6 of sine-wave as a reference signal (stored in a lookup table). This approach allows current sensorless strategies to generate gating signals for the appropriate power converter switches.

The modified SPWM switching scheme discussed in [13]-[16] was implemented in a unidirectional AC–DC three-phase, three-switch, 12-diode buck converter. The modified SPWM worked well when integrated with Flyback [13] and Sepic [14], [17] converters to achieve a wide range of input and output voltage. These studies prove that the modified SPWM achieves high-quality AC-current waveform, near-unity power factor, and system stability. These papers also show controllability of DC output voltage through modulation gain. However, without feedback control strategy, large starting current and voltage (during transient) result from large step-changes to the reference voltage because of the DC-side LC filter. In practice, a significant quantity of voltage drop is present when the modulation gain changes on the basis of theoretical calculation. This voltage drop is likewise caused by load changes due to the losses in the non-ideal converter elements, insulated-gate bipolar transistors (IGBT), and diodes. Another current sensorless approach proposed in [18] used PWM with input displacement factor correction in an AC–DC unidirectional six-switch six-diode buck converter. The paper simulated and experimented with modulation gain without feedback control and suggested the use of voltage feedback control to address the drawbacks of an uncompensated system.

The current paper proposes a simple and practical digital voltage feedback control that addresses the drawbacks of a modified SPWM. Unlike the typical controller that has inner (current) and outer (voltage) control loops, the single-input single-output (SISO) approach with minor-loop voltage feedback uses only one voltage sensor for the entire system. Simulations on MATLAB/Simulink verify the capability of and effectiveness in compensating start-up current/voltage and steady-state error. Fig. 1 shows the AC–DC buck converter with six-switch circuit configuration used.

The proposed controller has these features:

1. The controller has no current sensor.
2. The controller has only one DC-voltage sensor and updates the steady-state voltage. Change in the output voltage reference or load triggers the controller to update a new modulation gain ranging from 0 to 1. The controller is capable of compensating huge transient voltage/current and of achieving zero-steady-state-error output voltage.
3. The transient response can be controlled by tuning the proportional gain (K_p) only, which is an advantage over cascaded proportional-integral-derivative (PID) that tunes two or three parameters [15], [19].
4. The control principle is applicable to any AC–DC buck converters, e.g., three-switch 12-diode [13–16] or bidirectional three-phase [20].

II. Modified SPWM Strategy and System Configuration

A modified SPWM gating signal is generated by dividing a sine waveform (considered a reference signal) into six equal sections [21]; see Fig. 2(a). Fig. 2(b) shows a three-phase voltage waveform (reference signal) divided into six equal sections (I–VI) of the 360° main cycle. A similar pattern is repeated in each section; therefore, the analysis focuses on Section I only.

Two reference signals "A" and "C" were used for 0° to 60° and 120° to 180° sine waveforms, respectively. These signals were compared with triangular carrier signals "M" and "W" to produce modulated PWM patterns [13][16]. The reference signal for 90° to 120° (nearer to the sine-wave peak) was assumed to generate an "on" pulse.

Fig. 3 shows the circuit operation for modes 1, 2, and 3 (Section II). Modes 1 and 2 involve generating the modulation patterns T_a and T_b. Mode 3 provides a path for freewheeling current to flow at the DC side when both T_a and T_b are "off." The switch on the same leg with the T_{on} switch will be modulated into T_f (the pulse when neither T_a nor T_b or both are off). The commutating states of the converter switching period T for AC–DC operation are summarized in Table I.

III. Mathematical Analysis of Power Converter

The discussion focuses on designing a feedback controller for ac-dc power flow. Therefore, a mathematical analysis is done to prove the theory of the relationship between bridge voltage (V_L) and modulation index (M). The input phase voltage and the current waveforms can be expressed in term of phasors as follows,

$$V_a = V_m \angle -90^\circ ; \quad I_a = I_m \angle (\phi - 90^\circ) \tag{1}$$

$$V_b = V_m \angle (-\frac{2\pi}{3} - 90^\circ) ; I_b = I_m \angle (-\frac{2\pi}{3} + \phi - 90^\circ) \tag{2}$$

$$V_c = V_m \angle (\frac{2\pi}{3} - 90^\circ) \quad ; I_c = I_m \angle (\frac{2\pi}{3} + \phi - 90^\circ) \tag{3}$$

where V_m is the peak voltage, I_m is the peak current, and ϕ is the angle between the phase voltage and the current or displacement factor. From the phase voltage definitions of (1)–(3), the average bridge voltage $V_{L(average)}$ simplifies to (4) [15],[21].

$$V_{L(average)} = \frac{3}{2} V_m M \cos\varphi \tag{4}$$

M is the modulation gain, ranging from 0 to 1. If the power factor is considered unity, then

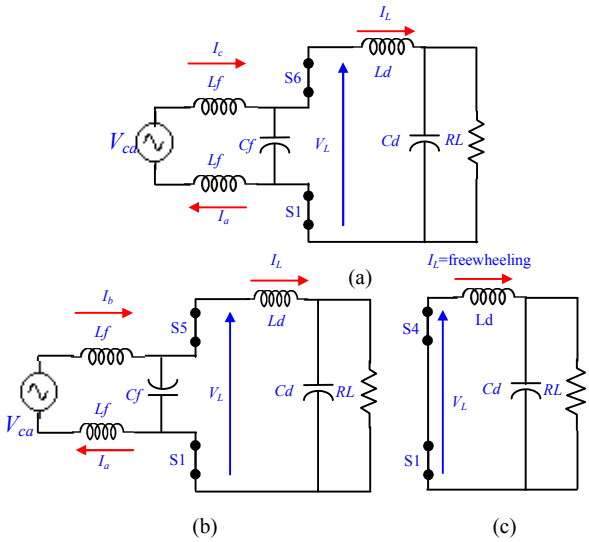

Fig. 3. Circuit operation based-on modified SPWM in (a) Mode 1, (b) Mode 2, and (c) Mode 3 at section II.

TABLE I

Switching-state of AC–DC Buck Converter for Sections I–VI.

	S1	S2	S3	S4	S5	S6
I	T_a	T_f	T_b	T_{off}	T_{on}	T_{off}
II	T_{on}	T_{off}	T_{off}	T_f	T_b	T_a
III	T_b	T_a	T_f	T_{off}	T_{off}	T_{on}
IV	T_{off}	T_{on}	T_{off}	T_a	T_f	T_b
V	T_f	T_b	T_a	T_{on}	T_{off}	T_{off}
VI	T_{off}	T_{off}	T_{on}	T_b	T_a	T_f

$$V_{L(average)} = \frac{3}{2} V_m M \tag{5}$$

Equation (5) shows V_L increasing linearly with M, proving that the DC output voltage can be controlled through M.

IV. Limits of the Modified SPWM without a Feedback Controller

The circuit with modified SPWM was simulated on MATLAB/Simulink. The configuration of the modified SPWM has LC input and output filters, 6 IGBTs, 24 diodes, and 1 freewheeling diode. The input filter resonant frequency was designed to be lower than the switching frequency to prevent circuit attenuation. The influence of the input filters (L_f and C_f) can be ignored if an appropriate input filter design is used [18], [22]–[24].

Table II lists the parameters of the power converter used in the simulation test. Fig. 4 shows the variation of V_o against M in simulation and in theory (see Eq. 5) and based on the parameters in Table II and the load resistance. The graph shows V_{dc} increasing linearly with M.

The modified SPWM design achieves near-unity power factor and provides steady-state system stability, but not the

TABLE II

PARAMETERS OF POWER CONVERTER

Switching Frequency f_s	19.8 kHz
Input Filter: L_f-R_f, C_f	1 mH to 0.5 Ω,1μF
Output Filter: L_d-R_d, C_d	6 mH to 0.5 Ω, 220 μF
Source Voltage Frequency f	50 Hz
Line-Neutral AC Voltage V_S	240 V_{rms}
Reference Voltage V_{ref}	400 V
Load Resistance R_L	20 Ω
Load Inductance L_L-R_L	160 mH series with 20 Ω

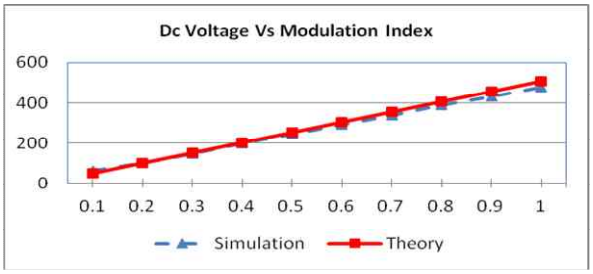

Fig. 4 Variation of output voltage against modulation gain, *M*.

desired transient response. Simulation tests in three transient conditions were done by step-changing the reference voltage from 60 V to 400 V with resistance and inductive loads and step-changing the load from 100 Ω to 20 Ω. Calculation for *M* was based on (5), and we assumed that the input and output powers are equal ($V_{L(average)} = V_o$).

Figs. 5(a–c) show the simulation results for phase-A voltage source $V_{L\text{-}N}$ and current source I_a, DC voltage output V_o, and inductor DC current I_L, and *M* in three transient cases. All the cases show high overshoot (more than 35%) in output voltage V_o and inductor current I_L, causing current stress on the semiconductors. In the third case, V_o and I_L oscillated more before settling down to stability. The settling time in the first and third cases was 25 ms, whereas in the second case was 60 ms. In addition, all cases had steady-state error because of non-ideal components (with losses). The drawbacks will be addressed by voltage feedback control.

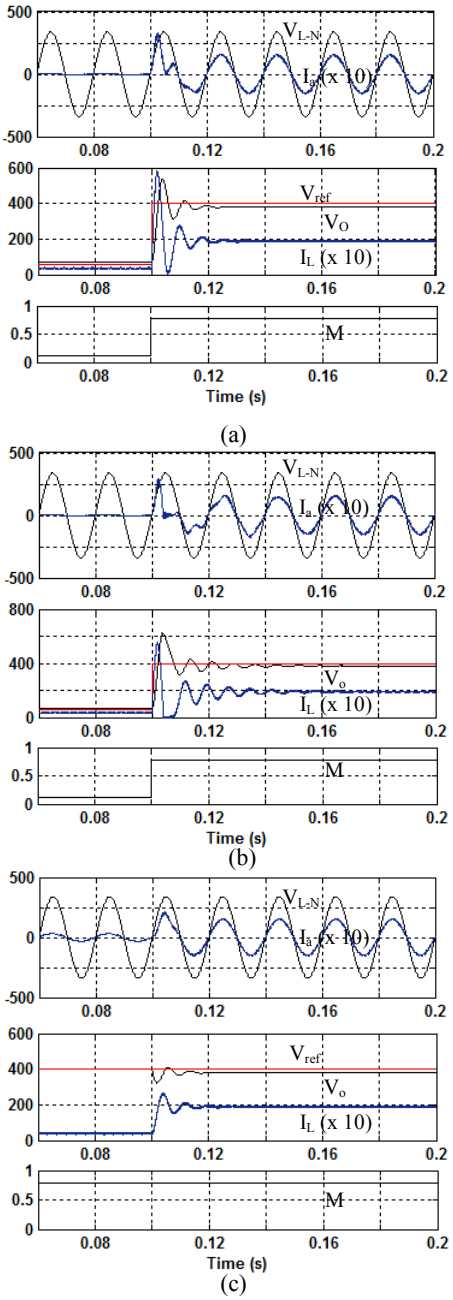

Fig. 5. Uncompensated step response (a) V_{ref} is changed in resistance load, (b) V_{ref} is changed in inductive load, and (c) Resistance load is changed.

V. FEEDBACK CONTROLLER DESIGN

A. Linear Model Design

The derivation of the transfer function in the ratio of output voltage to input voltage (V_o/V_{in}) was based on second-order resistor-inductor-capacitor circuit on the DC side. A linear and time-invariant system of the plant $G_p(s)$ was assumed.

$$G_p(s) = \frac{V_o(s)}{V_i(s)} = \frac{1}{L_d C_d s^2 + R_d C_d s + 1} \quad (6)$$

The open-loop step response of the system was simulated, with the open-loop poles located at −41.67+j869.39, the natural frequency at 870.39 rads^{-1}, and the damping ratio at 0.0479. A small damping ratio means oscillations and a huge percentage of overshoot in the output voltage of the uncompensated system. Thus, a controller is needed to change the location of the closed-loop dominant poles so that a good transient response and a zero steady-state error can be achieved.

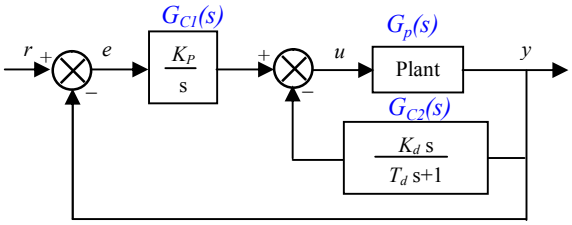

Fig. 6. A minor-loop feedback controller

Fig. 6 shows the proposed SISO approach with minor-loop voltage control. The controller has a derivative compensator $G_{C2}(s)$ in a minor loop around the plant and a proportional integral compensator $G_{C1}(s)$ in the forward path (an outer loop). The minor-loop feedback controller is a more suitable implementation than the conventional cascade PID is, particularly when step changes are present in the reference input. A cascade derivative action in a forward path will saturate plant input. Therefore, proportional-integral (PI) regulators are used more than cascaded PIDs in industries. However, the application of PI regulators alone does not greatly improve transient response, particularly when the disturbance is large.

The advantage of using the SISO approach with minor-loop voltage control is that the transient response of the system can be controlled by tuning only the proportional gain (K_p) to achieve the desired response through damping ratios 0 to 1 (and suitable values of T_d and K_d). Unlike other controllers (e.g., current controller, sliding mode controller, and fuzzy-plus-PI controller), the SISO approach also uses only one DC-voltage sensor to achieve zero-steady-state-error output voltage with high dynamic response, whether the disturbance is small or large.

B. Gain Tuning

The root locus technique was used in designing the value of K_p, K_d, and T_d because this technique is suitable for a SISO-type controller. This technique forces the root locus to pass through the desired closed-loop poles on the *s*-plane so that the response meets system performance specifications. The basic characteristic of the transient response of a closed-loop system closely relates to the location of the dominant closed-loop poles. Therefore, the designer/engineer should know how the closed-loop poles move on the *s*-plane (the root-locus) as the loop gain varies. The desired response specification can be met through an appropriate/suitable gain value. The gain-value tuning procedure is as follows:

a) Find the equivalent closed-loop transfer function (based on Fig. 6),

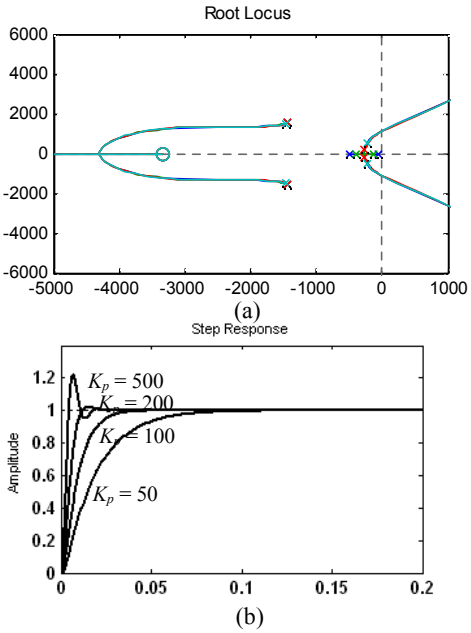

Fig. 7. Compensated system (a) root locus and closed-loop poles, (b) Step response; with different value of K_p

$$\frac{E(T_d s+1)}{As^4+Bs^3+Cs^2+Ds+E},$$

where $A= T_dL_dC_d$, $B= T_dR_dC_d+L_dC_d$, $C=T_d+R_dC_d+K_d$, $D=1+K_pT_d$, and $E=K_p$.

b) Choose value of T_d, where $-1/T_d$ is a location of zero and must be far to the left of the s-plane so that the influence of zero on the system can be ignored. T_d was chosen to be 0.0003.

c) K_d was selected to be about 10 times T_d to avoid the manipulated variable, $u(t)$, as an impulse function when a step-change is applied to the plant. As a result, $u(t)$ will become a sharp pulse function. K_d was fine-tuned through a study of the root locus shape. In this design, K_d was 0.002.

d) K_p is the system loop gain. This variable does not change the root locus shape. In the beginning, K_p was assumed to be 1.

Fig. 7(a) shows the root locus of the compensated system and the location of the closed-loop poles, with T_d=0.0003, K_d=0.002, and K_p = 50, 100, 200, 500. Fig. 7(b) shows the step response of the compensated system, which was stable as long as $0 < K_p < 2434$. The larger the K_p value, the more dominant poles reach the right side of the *s*-plane, thus increasing oscillations in the transient response. The linear-model-based proposed controller was then verified on a discrete model on the AC–DC buck converter system by using the modified SPWM switching technique.

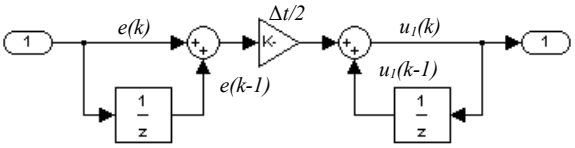

Fig. 8. An integral in discrete-domain.

C. Discrete Model

The control algorithm for the minor-loop voltage feedback controller in Fig. 6 was developed in a discrete model so that the algorithm can be implemented in digital signal processing (DSP). The algorithm can be expressed in discrete-time domain through the basic concept of integral. The integral term can be considered discrete via the following trapezoid approximation:

$$\int_{\tau}^{t} e(\tau)d\tau \cong \sum \frac{\Delta t}{2}[e(t_i)+e(t_{i-1})]. \quad (7)$$

The time relationship is $t_i = \Delta t*k$,
where Δt is the sampling time, and k is the discrete-time index (k=1,2,3….). Equation (7) can be computed in digital as continuous summation:

$$u_1(k) = u_1(k-1) + \frac{\Delta t}{2}[e(k)+e(k-1)]. \quad (8)$$

Fig. 8 is a block diagram for Eq. (8) drawn on MATLAB/Simulink.

The control block diagrams of Figs. 9(a, b), which show the outer-loop G_{C1} and the minor-loop G_{C2}, were modeled in time domain and discrete domain through integral concept.

According to Fig. 10(b), *u(k)* is calculated as

$$u(k) = u_1(k) + u_2(k), \quad (9)$$

where

$$u_1(k) = u_1(k-1) + \mathrm{K_P} * \frac{\Delta t}{2}[e(k)+e(k-1)] \quad (10)$$

$$e(k) = r(k) - y(k) \quad (11)$$

$$u_2(k) = sum(k-1) + \frac{\Delta t}{2}[e_1(k)+e_1(k-1)] + \frac{\mathrm{K_d}}{\mathrm{T_d}} * e_1(k-1) \quad (12)$$

$$e_1(k) = y(k) - \frac{1}{T_d} * sum(k-1) \quad (13)$$

$$sum(k) = sum(k-1) + \frac{\Delta t}{2}[e_1(k)+e_1(k-1)]. \quad (14)$$

Substituting (9) into (5) gives M as

$$M(k) = u(k)/1.5*V_P. \quad (15)$$

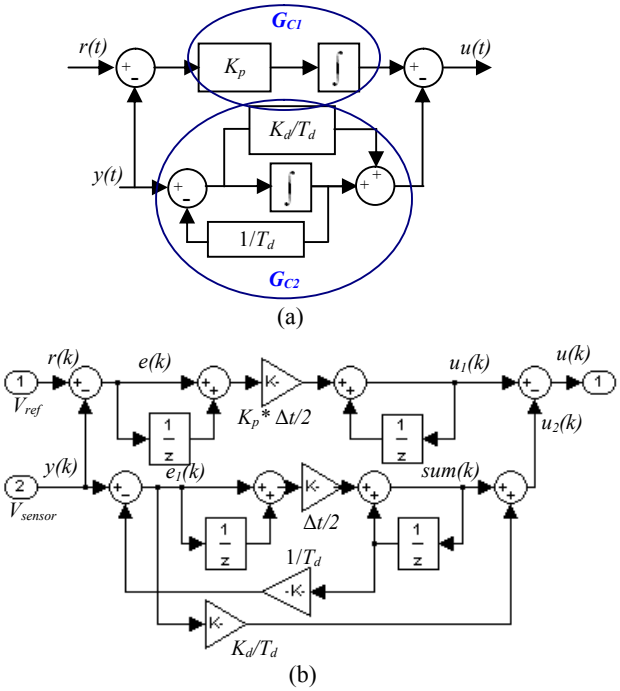

Fig. 9. Control block diagram of minor-loop, G_{c2} in (a) time-domain and, (b) discrete-domain.

Fig. 10 is the overall system and the proposed controller drawn on MATLAB/Simulink. V_o is the voltage measured across C_d. The output signal u is generated by the proposed control algorithm and is then multiplied with $1/1.5*V_p$ to obtain M (between 0 and 1). M is multiplied to the reference signals of the modified SPWM to generate the PWM of the three-phase AC–DC buck converter. The saturation block limits the value of M between 0 and 1 to protect the system from over-modulation.

VI. Simulation Results

The circuit with modified SPWM and discrete control was simulated on MATLAB/Simulink. The main objectives of the controller design are to obtain zero steady-state error in the output voltage (V_o=V_{ref}) despite any step-changes to the reference and load and to compensate for the huge voltage/current in the system. Results show that the controller is able to track the reference voltage with zero steady-state error while compensating for the huge starting voltage/current. However, in practice, tuning of a suitable K_p may be preferred to reduce current stress on the semiconductors during transients [15]. A fast and lightly damped system gives a fast step response but with the consequence of large-amplitude capacitor-charging current.

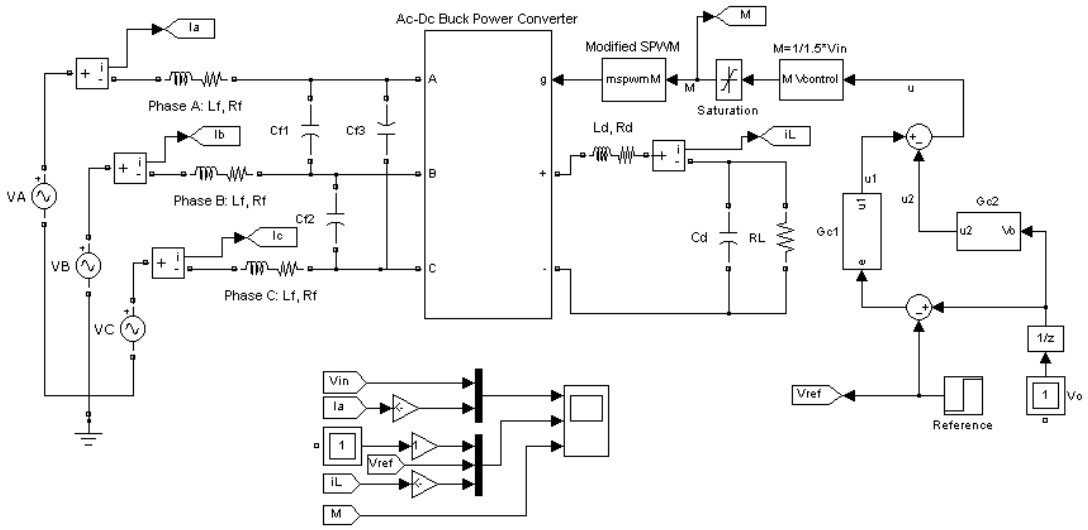

Fig. 10. The overall system and its control block diagram.

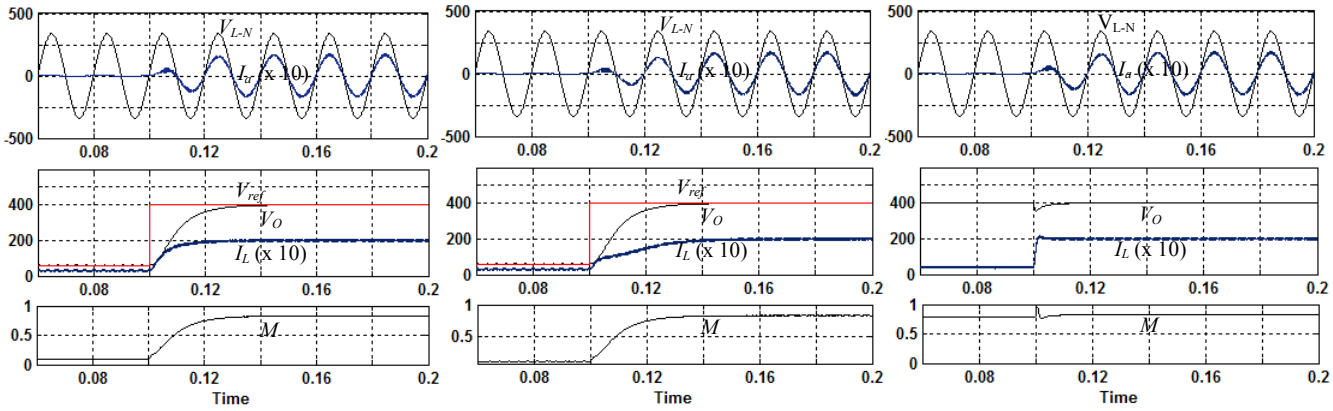

(a) (b) (c)

Fig. 11. Compensated step response. (a) V_{ref} is changed in resistance load; (b) V_{ref} is changed in inductive load; (c) resistance load is changed.

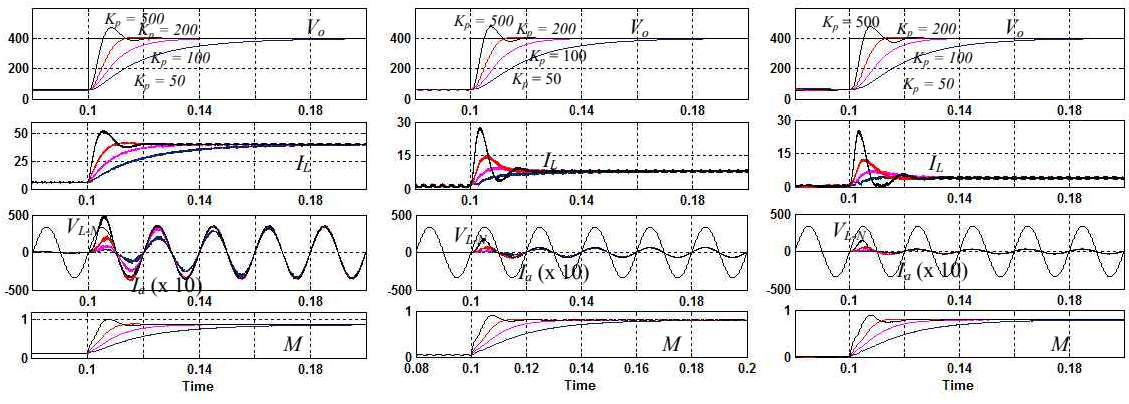

(a) (b) (c)

Fig. 12. Compensated step response of output voltage (V_o), inductor current (I_L), input voltage and current ($V_{L\text{-}N}$ and I_a), and modulation gain (M), when voltage reference (V_{ref}) changed at t = 0.1 s for (a) R_L=10 Ω, (b) R_L=50 Ω, and (c) R_L=100 Ω, for different values of K_p.

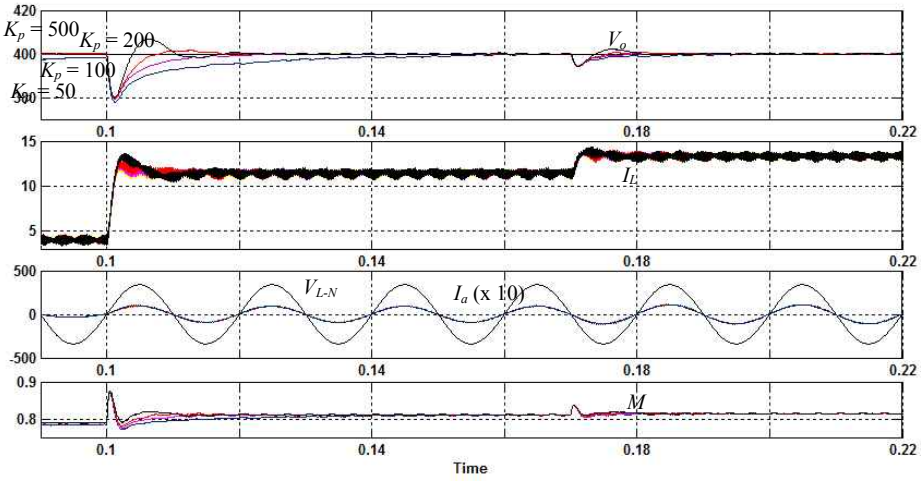

Fig. 13. Compensated step response of output voltage (V_o), inductor current (I_L), input voltage and current (V_{L-N} and I_a), and modulation gain (M), when resistance load changed (100Ω to 35Ω and then to 30Ω) at t=0.1s and 0.17s, for different value of K_p.

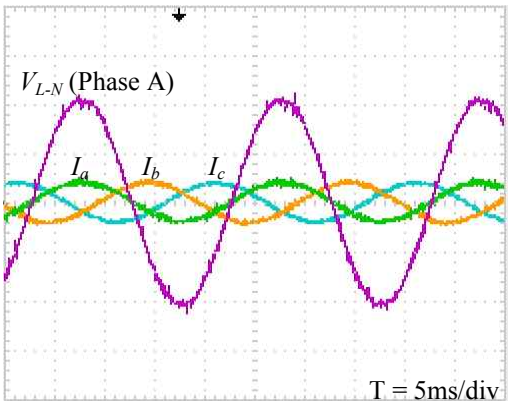

Fig. 14 Experimental results (steady-state) of the source voltage (50 V/div) for phase A, and the source current (5 A/div) for phases A, B, and C.

A. Analysis of the reference and load step changes

In the uncompensated tests, the tests on the control algorithm were done in three transient conditions: step-changing the reference voltage from 60 V to 400 V with resistance and inductive loads, and step-changing the load from 100 Ω to 20 Ω. The tests were done with feedback gain K_p=100. Figs. 11 (a–c) show the results for V_{L-N}, I_a, V_o, I_L, and M for the three cases. Compared with the uncompensated tests, V_o and I_L were reduced to almost zero in cases 1 and 2 and to below 5% in case 3. The settling time in the first and second cases was 25 ms and was improved greatly (10 ms) over the uncompensated system in the third case.

B. Analysis of the reference voltage step changes with K_p

Transient-response tests on reference-voltage step change were done for K_p = 50, 100, 200, and 500 and R_L=10, 50, and 100 Ω. Figs. 12 (a–c) show the results for V_{L-N}, I_a, V_o, I_L, and M against the values of R_L and K_p. The response was faster and the overshoot larger when K_p increased. The optimum design can be achieved by selecting a suitable gain for values of loads.

C. Analysis of the load-resistance step change against K_p

The transient-response tests on step change in load resistance were done by using small-value and large-value with controller gain, K_p = 50, 100, 200, and 500. The tests were done for load resistance R_L=100 Ω to 35 Ω at 0.1 s and R_L=35 Ω to 30 Ω at 0.17 s. Fig. 13 shows the results for voltage source (V_s), current source (I_s), voltage DC (load), inductor-current DC (I_L), and modulation gain, M against different values of load resistance and K_p. The controller is able to track the system to reach zero steady-state error faster with suitable controller gain in load disturbance tests (small and large signal disturbances).

VII. Experiment Results

The circuit with modified SPWM and its proposed discrete control algorithm were verified by a laboratory prototype. The input (L_f-C_f) and output filters (L_d-C_d) are 1 mH to 1 μF and 6 mH to 220 μF. The PWM and the proposed control algorithm were implemented in TMS320F28335 DSP. Fig. 14 shows the modified SPWM and the proposed control design achieving a steady-state, sinusoidal input current with near-unity power factor. The total harmonic distortion (THD) factor for input current was evaluated as THD = 3.5% (voltage supply, V_{L-N} = 3.3%). The power factor was evaluated as 0.98.

Transient tests were done in step disturbance load (case 1) and step changing of voltage reference (case 2). Figs. 15(a–b) show the results of case 1 (step-changing load from 100 Ω to50 Ω) for a system with and without feedback controller, respectively.

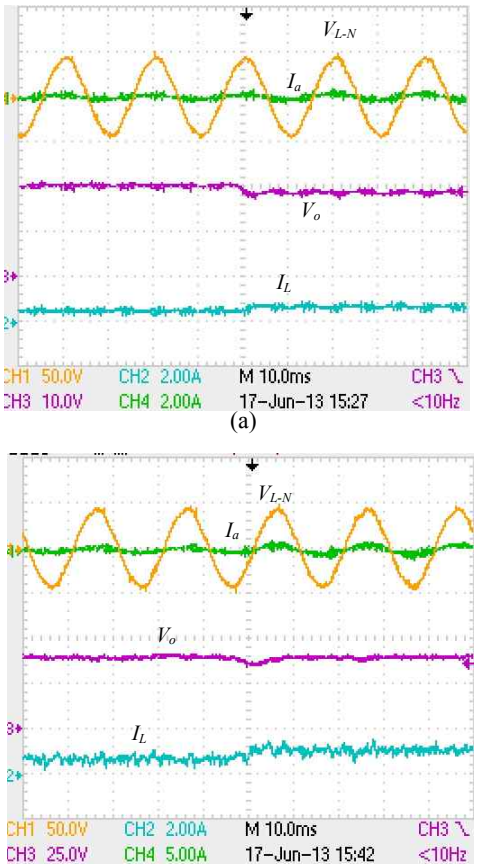

Fig. 15 Case 1: step-change of disturbance load (a) without controller and (b) with the proposed controller.

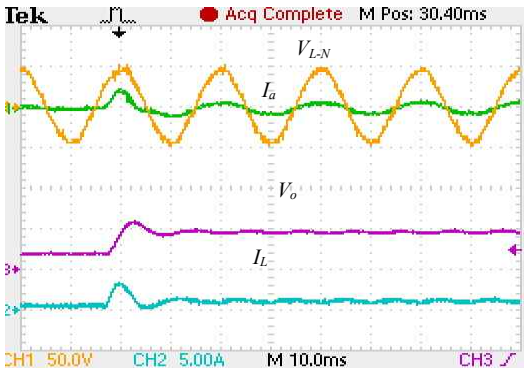

Fig. 16 Case 2: V_{ref} step-change for a system without controller.

The proposed controller can eliminate steady-state error with high dynamic response in output voltage compared with the system without controller (non-zero steady-state error).

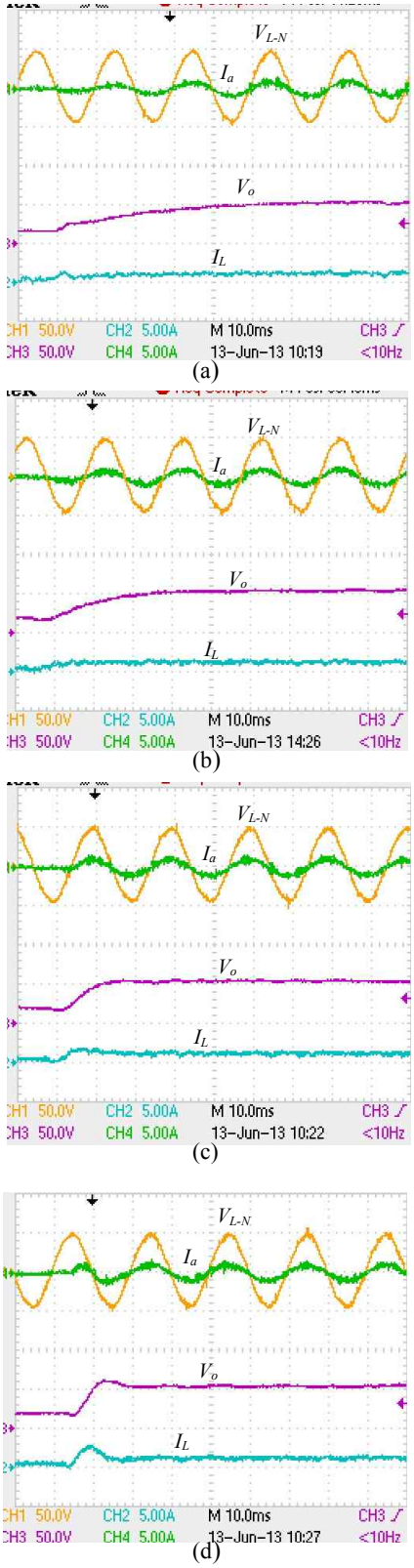

Fig. 17 V_{ref} step-change for a system with proposed controller with (a) K_p=50, (b) K_p=100, (c) K_p=200, and (d) K_P=300.

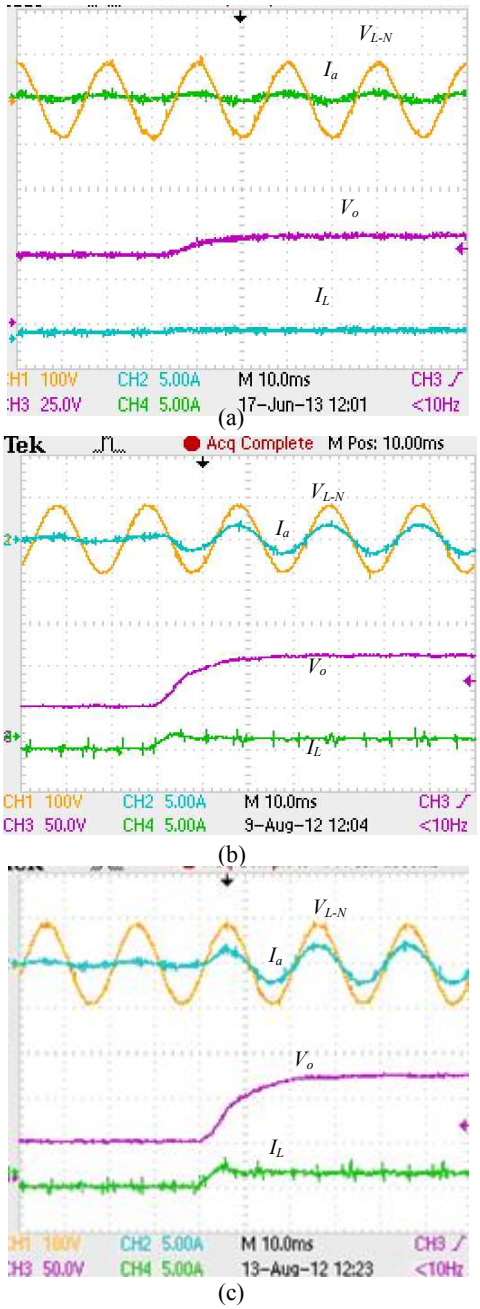

Fig. 18 V_{ref} step-change: (a) 40 V to 50 V, (b) 35 V to 95 V, and (c) 40 V to 120 V.

Case 2 tests were done by changing the V_{ref} from 20 V to 55 V. Fig. 16 shows that the system without feedback controller presents about 25% overshoot in DC output voltage and more than 100% overshoot produced in output current. The steady-state voltage is measured at 45 V and gives an offset value of 10 V because of the non-ideal converter elements. The results of the system with the proposed controller shown in Figs. 17(a)–(d) verify that the proposed controller can eliminate steady-state error from the output voltage. Our results confirm that the transient response can be controlled by tuning only the proportional gain K_p. The response is faster and the percentage overshoot (especially in I_L) is larger when the controller gain K_p is increased. Figs. 18 (a–c) show the step-response test with different values of V_{ref} for experimental verification. K_p is 100.

VIII. CONCLUSIONS

A discrete minor-loop voltage-feedback controller for a three-phase AC–DC buck converter has been presented. The controller addressed the drawbacks of modified SPWM by improving the steady-state and dynamic responses. The advantages of the proposed controller are ease of tuning and its use of only one sensor (DC voltage sensor). The theoretical strategy of this controller is based on a second-order linear model in Laplace form to diminish complex mathematical equations from system step-response analysis. The algorithm of the controller was modeled in discrete domain and then verified by MATLAB/Simulink simulation on an AC–DC buck-converter with modified SPWM switching technique. The results show that the proposed controller is able to compensate start-up current/voltage, reach zero steady-state error, and produce sinusoidal AC current with near-unity power factor in three transient cases: (1) the voltage reference changed for linear and non-linear loads, and the load changed. Transient analysis was also done with different controller gains to determine the controller that suits system application and requirement.

ACKNOWLEDGMENT

We would like to thank UTeM and MOHE for sponsoring the author[1]'s study. This project was funded by the University of Malaya (UM) Institute of Research Management and Monitoring (IPPP) through UM postgraduate-research grant PS113-2009C and PV037/2011B

.

REFERENCES

[1] T. Nussbaumer and J. W. Kolar, "Improving mains current quality for three-phase three-switch buck-type PWM rectifiers *IEEE Trans. Power Electron.,* Vol. 21, No. 4, pp. 967-973, Jul. 2006.

[2] T. Nussbaumer, M. L. Heldwin, G. Gong, S. D. Round and J. W. Kolar, "Comparison of prediction techniques to compensate time delays caused by digital control of a three-phase buck-type PWM rectifier system", *IEEE Trans. Industrial Electron.*, Vol. 55, No. 2, pp. 791-799, Feb. 2008.

[3] K. I. Hwu, H. W. Chen, and Y. T. Yau, "Fully digitalized implementation of PFC rectifier in CCM without ADC," *IEEE Trans. Power Electron*., Vol. 27, No. 9, pp. 4021–4029, Sep. 2012.

[4] M. Hao, L. Yunping and, C. Huiming, "A simplified algorithm for space vector modulation of three-phase voltage source PWM rectifier", *Power Electronics Specialists Conference (PECS)*, pp.3665-3670, 2004.
[5] S. Hiti, D. Borojevic, R. Ambatipudi, R. Zhang, and Y. Jiang, "Average current control of three-phase PWM boost rectifier", *Power Electronics Specialists Conference (PECS),* pp. 131-137, 1995.
[6] L. Malesani and P. Tenti, "A novel hysteresis control method for current-controlled voltage-source PWM inverters with constant modulation frequency", *IEEE Trans. Industrial Appl.,* Vol. 26, No. 1, pp. 88-92, Feb. 1990.
[7] L. Dalessandro, U. Drofenik, S.D. Round and J.W. Kolar, "A novel hysteresis current control for three-phase three-level PWM rectifiers", *Applied Power Electronics Conference and Exposition (APEC),* pp. 501 – 507, 2005.
[8] Y. Rong, C. Li, and Q. Ding, "An adaptive harmonic detection and a novel current control strategy for unified power quality conditioner", *Simulation Modelling Practice and Theory,* Vol. 17, pp. 955–966, 2009.
[9] IEEE Recommended Practices and Requirements for Harmonics Control in Electric Power Systems, IEEE std. 519, 1992.
[10] Electromagnetic Compatibility (EMC)-Part 3: Limits-Section 2: Limits for Harmonic Current Emissions (Equipment Input Current Emissions (Equipment Input Current < 16A per Phase), IEC1000-3-2 Doc., 1995.
[11] B. Singh, B. N. Singh, A. Chandra, K. Al-Haddad, A. Pandey and D. P. Kothari, "A review of three-phase improved power quality AC–DC converters", *IEEE Trans. Ind. Electron*., Vol. 51, No. 3, pp. 641-660, Jun. 2004.
[12] J. R. Rodríguez, J. W. Dixon, J. R. Espinoza, and P. Lezana, "PWM regenerative rectifiers: State of the art", *IEEE Trans. Ind. Electron*., Vol. 52, No. 1, pp. 5-22, Feb. 2005.
[13] A. M. Omar and N. A. Rahim, "FPGA-based ASIC design of the three-phase synchronous PWM flyback converter," *in Electronic Power Application*, pp. 263-268, 2003.
[14] S. S. Raihan, and N. A. Rahim, "FPGA-based PWM for three-phase SEPIC rectifier," *IEICE Electron. Express*, Vol. 7, No. 18, pp. 1335–1341, 2010.
[15] T. C. Green, M. H. Taha, N. A. Rahim, and B. W. Williams, "Three-phase step-down reversible AC–DC power converter", *IEEE Trans. Power Electron*., Vol. 12, No. 2, pp. 319-324, Mar. 1997.
[16] N. A. Rahim, T. C. Green, and B. W. Williams, "PWM ASIC design for the three-phase bi-directional buck converter," *International Journal of Electronics*, Vol. 81, No. 5, pp. 603-615, 1996.
[17] S. R. S. Raihan and N. A. Rahim, "Comparative analysis of three-phase AC–DC converters using HIL-simulation," *Journal of Power Electronics*, Vol. 13, No. 1, pp. 104-112, Jan. 2013.
[18] M. Milanovic, and P. Slibar, "IDF ccrrection based PWM algorithm for a three-phase AC–DC buck converter", *IEEE Trans. Industrial Electron.,* Vol. 58, No. 8, pp. 3308-3316, Aug. 2011.
[19] A. S. Samosir, and A. H. M. Yatim, "Dynamic evolution control for synchronous buck DC-DC converter: Theory, model and simulation", *Simulation Modelling Practice and Theory*, Vol. 18, pp. 663–676, 2010.
[20] L. S. Yang, T. J. Liang, and J. F. Chen, "Three-phase ac/DC buck converter with bidirectional capability", *Power Electronics Specialists Conference (PECS),* pp. 1–6, 2006.
[21] H. M. Rashid, *Power Electronics: Circuits, Devices And Applications,* 3rd edition, United States of America: Pearson Prentice Hall, 2004, pp. 248.
[22] A.-M. Majed, T. C. Green, and B. W. Williams, "Low EMI 3-phase AC/DC converter with controllable displacement factor," *Conf. Rec. Power Quality*, 1992.
[23] P. Lezana, J. R. Rodríguez, M.A. Pérez, and J. R. Espinoza, "Input current harmonics in a regenerative multicell inverter with single-phase PWM rectifiers", *IEEE Trans. Industrial Electron*, Vol. 56, No. 2, pp. 408-417, Feb. 2009.
[24] N. Vázquez, H. Rodríguez, C. Hernández, E. Rodríguez, and J. Arau, "Three-phase rectifier with active current injection and high efficiency," *IEEE Trans. Ind. Electron.,* Vol. 56, No. 1, pp. 110-119, Jan. 2009.
[25] D. Casadei, G. Sera, A. Tani, and L. Zarri, "Optimal use of zero vectors for minimizing the output current distortion in matrix converter," *IEEE Trans. Ind. Electron.,* Vol. 56, No. 2, pp. 326-336, Feb. 2009.

Azrita Alias was born in Terengganu, Malaysia, in 1978. She received her B. Eng in Electrical (Control and Instrumentation) (Hons) and M. Eng (Electrical) from the Universiti Teknologi Malaysia, in 2000 and 2003, respectively. She is currently working toward her PhD at the University of Malaya, Kuala Lumpur, Malaysia. She is a lecturer at the Faculty of Electrical Engineering, Universiti Teknikal Malaysia Melaka (UTeM).

Nasrudin Abd. Rahim was born in Johor, Malaysia, in 1960. He received his BS (with Honors) and MS from the University of Strathclyde, Glasgow, United Kingdom, and his PhD from Heriot-Watt University, Edinburgh, United Kingdom, in 1995. He is currently a professor at the University of Malaya, Kuala Lumpur, Malaysia, where he is also the director of the University of Malaya Power Energy Dedicated Advanced Centre (UMPEDAC). At present he is an Adjunct Professor at King Abdulaziz University, Jeddah, Saudi Arabia. Professor Rahim is a senior member of IEEE, a fellow of the Institution of Engineering and Technology, United Kingdom, and a fellow of the Academy of Sciences Malaysia. He is also a chartered engineer.

Mohamed Azlan Hussain joined the Department of Chemical Engineering, University of Malaya in 1987 as a lecturer and obtained his PhD in Chemical Engineering from Imperial College, London in 1996. He is a member of the American Institute of Chemical Engineers and British

Institute of Chemical Engineers. At present, he is holding the post of professor in the Department of Chemical Engineering. His main research interests are in modeling, process controls, nonlinear control systems analysis, and applications of artificial intelligence techniques in engineering systems. At present, he has published more than 250 papers in book chapters, journals, and conferences within these areas. He has also published and edited a book on "Application of Neural Networks and other learning Technologies in Process Engineering" published by Imperial College Press in 2001.